

Model-independent measurement of t -channel single top quark production in $p\bar{p}$ collisions at $\sqrt{s} = 1.96$ TeV

V.M. Abazov,³⁵ B. Abbott,⁷³ B.S. Acharya,²⁹ M. Adams,⁴⁹ T. Adams,⁴⁷ G.D. Alexeev,³⁵ G. Alkhazov,³⁹ A. Alton^{a,61} G. Alverson,⁶⁰ G.A. Alves,² L.S. Ancu,³⁴ M. Aoki,⁴⁸ M. Arov,⁵⁸ A. Askew,⁴⁷ B. Åsman,⁴¹ O. Atramentov,⁶⁵ C. Avila,⁸ J. BackusMayes,⁸⁰ F. Badaud,¹³ L. Bagby,⁴⁸ B. Baldin,⁴⁸ D.V. Bandurin,⁴⁷ S. Banerjee,²⁹ E. Barberis,⁶⁰ P. Baringer,⁵⁶ J. Barreto,³ J.F. Bartlett,⁴⁸ U. Bassler,¹⁸ V. Bazterra,⁴⁹ S. Beale,⁶ A. Bean,⁵⁶ M. Begalli,³ M. Begel,⁷¹ C. Belanger-Champagne,⁴¹ L. Bellantoni,⁴⁸ S.B. Beri,²⁷ G. Bernardi,¹⁷ R. Bernhard,²² I. Bertram,⁴² M. Besançon,¹⁸ R. Beuselinck,⁴³ V.A. Bezzubov,³⁸ P.C. Bhat,⁴⁸ V. Bhatnagar,²⁷ G. Blazey,⁵⁰ S. Blessing,⁴⁷ K. Bloom,⁶⁴ A. Boehnlein,⁴⁸ D. Boline,⁷⁰ E.E. Boos,³⁷ G. Borissov,⁴² T. Bose,⁵⁹ A. Brandt,⁷⁶ O. Brandt,²³ R. Brock,⁶² G. Brooijmans,⁶⁸ A. Bross,⁴⁸ D. Brown,¹⁷ J. Brown,¹⁷ X.B. Bu,⁴⁸ M. Buehler,⁷⁹ V. Buescher,²⁴ V. Bunichev,³⁷ S. Burdin^{b,42} T.H. Burnett,⁸⁰ C.P. Buszello,⁴¹ B. Calpas,¹⁵ E. Camacho-Pérez,³² M.A. Carrasco-Lizarraga,⁵⁶ B.C.K. Casey,⁴⁸ H. Castilla-Valdez,³² S. Chakrabarti,⁷⁰ D. Chakraborty,⁵⁰ K.M. Chan,⁵⁴ A. Chandra,⁷⁸ G. Chen,⁵⁶ S. Chevalier-Théry,¹⁸ D.K. Cho,⁷⁵ S.W. Cho,³¹ S. Choi,³¹ B. Choudhary,²⁸ S. Cihangir,⁴⁸ D. Claes,⁶⁴ J. Clutter,⁵⁶ J. Cochran,⁵⁵ M. Cooke,⁴⁸ W.E. Cooper,⁴⁸ M. Corcoran,⁷⁸ F. Couderc,¹⁸ M.-C. Cousinou,¹⁵ A. Croc,¹⁸ D. Cutts,⁷⁵ A. Das,⁴⁵ G. Davies,⁴³ K. De,⁷⁶ S.J. de Jong,³⁴ E. De La Cruz-Burelo,³² F. Déliot,¹⁸ M. Demarteau,⁴⁸ R. Demina,⁶⁹ D. Denisov,⁴⁸ S.P. Denisov,³⁸ S. Desai,⁴⁸ C. Deterre,¹⁸ K. DeVaughan,⁶⁴ H.T. Diehl,⁴⁸ M. Diesburg,⁴⁸ A. Dominguez,⁶⁴ T. Dorland,⁸⁰ A. Dubey,²⁸ L.V. Dudko,³⁷ D. Duggan,⁶⁵ A. Duperrin,¹⁵ S. Dutt,²⁷ A. Dyshkant,⁵⁰ M. Eads,⁶⁴ D. Edmunds,⁶² P. Eller^{h,49} J. Ellison,⁴⁶ V.D. Elvira,⁴⁸ Y. Enari,¹⁷ H. Evans,⁵² A. Evdokimov,⁷¹ V.N. Evdokimov,³⁸ G. Facini,⁶⁰ T. Ferbel,⁶⁹ F. Fiedler,²⁴ F. Filthaut,³⁴ W. Fisher,⁶² H.E. Fisk,⁴⁸ C. Focke^{h,49} M. Fortner,⁵⁰ H. Fox,⁴² S. Fuess,⁴⁸ A. Garcia-Bellido,⁶⁹ V. Gavrilov,³⁶ P. Gay,¹³ W. Geng,^{15,62} D. Gerbaudo,⁶⁶ C.E. Gerber,⁴⁹ Y. Gershtein,⁶⁵ G. Ginther,^{48,69} G. Golovanov,³⁵ A. Goussiou,⁸⁰ P.D. Grannis,⁷⁰ S. Greder,¹⁹ H. Greenlee,⁴⁸ Z.D. Greenwood,⁵⁸ E.M. Gregores,⁴ G. Grenier,²⁰ Ph. Gris,¹³ J.-F. Grivaz,¹⁶ A. Grohsjean,¹⁸ S. Grünendahl,⁴⁸ M.W. Grünewald,³⁰ T. Guillemin,¹⁶ F. Guo,⁷⁰ G. Gutierrez,⁴⁸ P. Gutierrez,⁷³ A. Haas^{c,68} S. Hagopian,⁴⁷ J. Haley,⁶⁰ L. Han,⁷ K. Harder,⁴⁴ A. Harel,⁶⁹ J.M. Hauptman,⁵⁵ J. Hays,⁴³ T. Head,⁴⁴ T. Hebbeker,²¹ D. Hedin,⁵⁰ H. Hegab,⁷⁴ A.P. Heinson,⁴⁶ U. Heintz,⁷⁵ C. Hensel,²³ I. Heredia-De La Cruz,³² K. Herner,⁶¹ G. Hesketh^{d,44} M.D. Hildreth,⁵⁴ R. Hirosky,⁷⁹ T. Hoang,⁴⁷ J.D. Hobbs,⁷⁰ B. Hoeneisen,¹² M. Hohlfeld,²⁴ Z. Hubacek,^{10,18} N. Huske,¹⁷ V. Hynek,¹⁰ I. Iashvili,⁶⁷ R. Illingworth,⁴⁸ A.S. Ito,⁴⁸ S. Jabeen,⁷⁵ M. Jaffré,¹⁶ D. Jamin,¹⁵ A. Jayasinghe,⁷³ R. Jesik,⁴³ K. Johns,⁴⁵ M. Johnson,⁴⁸ D. Johnston,⁶⁴ A. Jonckheere,⁴⁸ P. Jonsson,⁴³ J. Joshi,²⁷ A.W. Jung,⁴⁸ A. Juste,⁴⁰ K. Kaadze,⁵⁷ E. Kajfasz,¹⁵ D. Karmanov,³⁷ P.A. Kasper,⁴⁸ I. Katsanos,⁶⁴ R. Kehoe,⁷⁷ S. Kermiche,¹⁵ N. Khalatyan,⁴⁸ A. Khanov,⁷⁴ A. Kharchilava,⁶⁷ Y.N. Kharzheev,³⁵ D. Khatidze,⁷⁵ M.H. Kirby,⁵¹ J.M. Kohli,²⁷ A.V. Kozelov,³⁸ J. Kraus,⁶² S. Kulikov,³⁸ A. Kumar,⁶⁷ A. Kupco,¹¹ T. Kurča,²⁰ V.A. Kuzmin,³⁷ J. Kvita,⁹ S. Lammers,⁵² G. Landsberg,⁷⁵ P. Lebrun,²⁰ H.S. Lee,³¹ S.W. Lee,⁵⁵ W.M. Lee,⁴⁸ J. Lellouch,¹⁷ L. Li,⁴⁶ Q.Z. Li,⁴⁸ S.M. Lietti,⁵ J.K. Lim,³¹ D. Lincoln,⁴⁸ J. Linnemann,⁶² V.V. Lipaev,³⁸ R. Lipton,⁴⁸ Y. Liu,⁷ Z. Liu,⁶ A. Lobodenko,³⁹ M. Lokajicek,¹¹ R. Lopes de Sa,⁷⁰ H.J. Lubatti,⁸⁰ R. Luna-Garcia^{e,32} A.L. Lyon,⁴⁸ A.K.A. Maciel,² D. Mackin,⁷⁸ R. Madar,¹⁸ R. Magaña-Villalba,³² S. Malik,⁶⁴ V.L. Malyshev,³⁵ Y. Maravin,⁵⁷ J. Martínez-Ortega,³² R. McCarthy,⁷⁰ C.L. McGivern,⁵⁶ M.M. Meijer,³⁴ A. Melnitchouk,⁶³ D. Menezes,⁵⁰ P.G. Mercadante,⁴ M. Merkin,³⁷ A. Meyer,²¹ J. Meyer,²³ F. Miconi,¹⁹ N.K. Mondal,²⁹ G.S. Muanza,¹⁵ M. Mulhearn,⁷⁹ E. Nagy,¹⁵ M. Naimuddin,²⁸ M. Narain,⁷⁵ R. Nayyar,²⁸ H.A. Neal,⁶¹ J.P. Negret,⁸ P. Neustroev,³⁹ S.F. Novaes,⁵ T. Nunnemann,²⁵ G. Obrant,³⁹ J. Orduna,⁷⁸ N. Osman,¹⁵ J. Osta,⁵⁴ G.J. Otero y Garzón,¹ M. Padilla,⁴⁶ A. Pal,⁷⁶ N. Parashar,⁵³ V. Parihar,⁷⁵ S.K. Park,³¹ J. Parsons,⁶⁸ R. Partridge^{c,75} N. Parua,⁵² A. Patwa,⁷¹ B. Penning,⁴⁸ M. Perfilov,³⁷ K. Peters,⁴⁴ Y. Peters,⁴⁴ K. Petridis,⁴⁴ G. Petrillo,⁶⁹ P. Pétrouff,¹⁶ R. Piegaia,¹ J. Piper,⁶² M.-A. Pleier,⁷¹ P.L.M. Podesta-Lerma^{f,32} V.M. Podstavkov,⁴⁸ P. Polozov,³⁶ A.V. Popov,³⁸ M. Prewitt,⁷⁸ D. Price,⁵² N. Prokopenko,³⁸ S. Protopopescu,⁷¹ J. Qian,⁶¹ A. Quadt,²³ B. Quinn,⁶³ M.S. Rangel,² K. Ranjan,²⁸ P.N. Ratoff,⁴² I. Razumov,³⁸ P. Renkel,⁷⁷ M. Rijssenbeek,⁷⁰ I. Ripp-Baudot,¹⁹ F. Rizatdinova,⁷⁴ M. Rominsky,⁴⁸ A. Ross,⁴² C. Royon,¹⁸ P. Rubinov,⁴⁸ R. Ruchti,⁵⁴ G. Safronov,³⁶ G. Sajot,¹⁴ P. Salcido,⁵⁰ A. Sánchez-Hernández,³² M.P. Sanders,²⁵ B. Sanghi,⁴⁸ A.S. Santos,⁵ G. Savage,⁴⁸ L. Sawyer,⁵⁸ T. Scanlon,⁴³ R.D. Schamberger,⁷⁰ Y. Scheglov,³⁹ H. Schellman,⁵¹ T. Schliephake,²⁶ S. Schlobohm,⁸⁰ C. Schwanenberger,⁴⁴ R. Schwienhorst,⁶² J. Sekaric,⁵⁶ H. Severini,⁷³ E. Shabalina,²³ V. Shary,¹⁸ A.A. Shchukin,³⁸ R.K. Shivpuri,²⁸ V. Simak,¹⁰ V. Sirotenko,⁴⁸ P. Skubic,⁷³ P. Slattey,⁶⁹ D. Smirnov,⁵⁴ K.J. Smith,⁶⁷ G.R. Snow,⁶⁴ J. Snow,⁷²

S. Snyder,⁷¹ S. Söldner-Rembold,⁴⁴ L. Sonnenschein,²¹ K. Soustruznik,⁹ J. Stark,¹⁴ V. Stolin,³⁶ D.A. Stoyanova,³⁸ M. Strauss,⁷³ D. Strom,⁴⁹ L. Stutte,⁴⁸ L. Suter,⁴⁴ P. Svoisky,⁷³ M. Takahashi,⁴⁴ A. Tanasijczuk,¹ W. Taylor,⁶ M. Titov,¹⁸ V.V. Tokmenin,³⁵ N. Triplett,⁵⁵ Y.-T. Tsai,⁶⁹ D. Tsybychev,⁷⁰ B. Tuchming,¹⁸ C. Tully,⁶⁶ L. Uvarov,³⁹ S. Uvarov,³⁹ S. Uzunyan,⁵⁰ R. Van Kooten,⁵² W.M. van Leeuwen,³³ N. Varelas,⁴⁹ E.W. Varnes,⁴⁵ I.A. Vasilyev,³⁸ P. Verdier,²⁰ L.S. Vertogradov,³⁵ M. Verzocchi,⁴⁸ M. Vesterinen,⁴⁴ D. Vilanova,¹⁸ P. Vokac,¹⁰ H.D. Wahl,⁴⁷ M.H.L.S. Wang,⁶⁹ J. Warchol,⁵⁴ G. Watts,⁸⁰ M. Wayne,⁵⁴ M. Weber,^{9, 48} L. Welty-Rieger,⁵¹ A. White,⁷⁶ D. Wicke,²⁶ M.R.J. Williams,⁴² G.W. Wilson,⁵⁶ M. Wobisch,⁵⁸ D.R. Wood,⁶⁰ T.R. Wyatt,⁴⁴ Y. Xie,⁴⁸ C. Xu,⁶¹ S. Yacoob,⁵¹ R. Yamada,⁴⁸ W.-C. Yang,⁴⁴ T. Yasuda,⁴⁸ Y.A. Yatsunenko,³⁵ Z. Ye,⁴⁸ H. Yin,⁴⁸ K. Yip,⁷¹ S.W. Youn,⁴⁸ J. Yu,⁷⁶ S. Zelitch,⁷⁹ T. Zhao,⁸⁰ B. Zhou,⁶¹ J. Zhu,⁶¹ M. Zielinski,⁶⁹ D. Zieminska,⁵² and L. Zivkovic⁷⁵

(The D0 Collaboration*)

¹Universidad de Buenos Aires, Buenos Aires, Argentina

²LAFEX, Centro Brasileiro de Pesquisas Físicas, Rio de Janeiro, Brazil

³Universidade do Estado do Rio de Janeiro, Rio de Janeiro, Brazil

⁴Universidade Federal do ABC, Santo André, Brazil

⁵Instituto de Física Teórica, Universidade Estadual Paulista, São Paulo, Brazil

⁶Simon Fraser University, Vancouver, British Columbia, and York University, Toronto, Ontario, Canada

⁷University of Science and Technology of China, Hefei, People's Republic of China

⁸Universidad de los Andes, Bogotá, Colombia

⁹Charles University, Faculty of Mathematics and Physics,

Center for Particle Physics, Prague, Czech Republic

¹⁰Czech Technical University in Prague, Prague, Czech Republic

¹¹Center for Particle Physics, Institute of Physics,
Academy of Sciences of the Czech Republic, Prague, Czech Republic

¹²Universidad San Francisco de Quito, Quito, Ecuador

¹³LPC, Université Blaise Pascal, CNRS/IN2P3, Clermont, France

¹⁴LPSC, Université Joseph Fourier Grenoble 1, CNRS/IN2P3,

Institut National Polytechnique de Grenoble, Grenoble, France

¹⁵CPPM, Aix-Marseille Université, CNRS/IN2P3, Marseille, France

¹⁶LAL, Université Paris-Sud, CNRS/IN2P3, Orsay, France

¹⁷LPNHE, Universités Paris VI and VII, CNRS/IN2P3, Paris, France

¹⁸CEA, Irfu, SPP, Saclay, France

¹⁹IPHC, Université de Strasbourg, CNRS/IN2P3, Strasbourg, France

²⁰IPNL, Université Lyon 1, CNRS/IN2P3, Villeurbanne, France and Université de Lyon, Lyon, France

²¹III. Physikalisches Institut A, RWTH Aachen University, Aachen, Germany

²²Physikalisches Institut, Universität Freiburg, Freiburg, Germany

²³II. Physikalisches Institut, Georg-August-Universität Göttingen, Göttingen, Germany

²⁴Institut für Physik, Universität Mainz, Mainz, Germany

²⁵Ludwig-Maximilians-Universität München, München, Germany

²⁶Fachbereich Physik, Bergische Universität Wuppertal, Wuppertal, Germany

²⁷Panjab University, Chandigarh, India

²⁸Delhi University, Delhi, India

²⁹Tata Institute of Fundamental Research, Mumbai, India

³⁰University College Dublin, Dublin, Ireland

³¹Korea Detector Laboratory, Korea University, Seoul, Korea

³²CINVESTAV, Mexico City, Mexico

³³FOM-Institute NIKHEF and University of Amsterdam/NIKHEF, Amsterdam, The Netherlands

³⁴Radboud University Nijmegen/NIKHEF, Nijmegen, The Netherlands

³⁵Joint Institute for Nuclear Research, Dubna, Russia

³⁶Institute for Theoretical and Experimental Physics, Moscow, Russia

³⁷Moscow State University, Moscow, Russia

³⁸Institute for High Energy Physics, Protvino, Russia

³⁹Petersburg Nuclear Physics Institute, St. Petersburg, Russia

⁴⁰Institució Catalana de Recerca i Estudis Avançats (ICREA) and Institut de Física d'Altes Energies (IFAE), Barcelona, Spain

⁴¹Stockholm University, Stockholm and Uppsala University, Uppsala, Sweden

⁴²Lancaster University, Lancaster LA1 4YB, United Kingdom

⁴³Imperial College London, London SW7 2AZ, United Kingdom

⁴⁴The University of Manchester, Manchester M13 9PL, United Kingdom

⁴⁵University of Arizona, Tucson, Arizona 85721, USA

⁴⁶University of California Riverside, Riverside, California 92521, USA

⁴⁷Florida State University, Tallahassee, Florida 32306, USA

⁴⁸Fermi National Accelerator Laboratory, Batavia, Illinois 60510, USA

- ⁴⁹University of Illinois at Chicago, Chicago, Illinois 60607, USA
⁵⁰Northern Illinois University, DeKalb, Illinois 60115, USA
⁵¹Northwestern University, Evanston, Illinois 60208, USA
⁵²Indiana University, Bloomington, Indiana 47405, USA
⁵³Purdue University Calumet, Hammond, Indiana 46323, USA
⁵⁴University of Notre Dame, Notre Dame, Indiana 46556, USA
⁵⁵Iowa State University, Ames, Iowa 50011, USA
⁵⁶University of Kansas, Lawrence, Kansas 66045, USA
⁵⁷Kansas State University, Manhattan, Kansas 66506, USA
⁵⁸Louisiana Tech University, Ruston, Louisiana 71272, USA
⁵⁹Boston University, Boston, Massachusetts 02215, USA
⁶⁰Northeastern University, Boston, Massachusetts 02115, USA
⁶¹University of Michigan, Ann Arbor, Michigan 48109, USA
⁶²Michigan State University, East Lansing, Michigan 48824, USA
⁶³University of Mississippi, University, Mississippi 38677, USA
⁶⁴University of Nebraska, Lincoln, Nebraska 68588, USA
⁶⁵Rutgers University, Piscataway, New Jersey 08855, USA
⁶⁶Princeton University, Princeton, New Jersey 08544, USA
⁶⁷State University of New York, Buffalo, New York 14260, USA
⁶⁸Columbia University, New York, New York 10027, USA
⁶⁹University of Rochester, Rochester, New York 14627, USA
⁷⁰State University of New York, Stony Brook, New York 11794, USA
⁷¹Brookhaven National Laboratory, Upton, New York 11973, USA
⁷²Langston University, Langston, Oklahoma 73050, USA
⁷³University of Oklahoma, Norman, Oklahoma 73019, USA
⁷⁴Oklahoma State University, Stillwater, Oklahoma 74078, USA
⁷⁵Brown University, Providence, Rhode Island 02912, USA
⁷⁶University of Texas, Arlington, Texas 76019, USA
⁷⁷Southern Methodist University, Dallas, Texas 75275, USA
⁷⁸Rice University, Houston, Texas 77005, USA
⁷⁹University of Virginia, Charlottesville, Virginia 22901, USA
⁸⁰University of Washington, Seattle, Washington 98195, USA
- (Dated: May 13, 2011)

We present a model-independent measurement of t -channel electroweak production of single top quarks in $p\bar{p}$ collisions at $\sqrt{s} = 1.96$ TeV. Using 5.4 fb^{-1} of integrated luminosity collected by the D0 detector at the Fermilab Tevatron Collider, and selecting events containing an isolated electron or muon, missing transverse energy and one or two jets originating from the fragmentation of b quarks, we measure a cross section $\sigma(p\bar{p} \rightarrow tqb + X) = 2.90 \pm 0.59$ (stat + syst) pb for a top quark mass of 172.5 GeV. The probability of the background to fluctuate and produce a signal as large as the one observed is 1.6×10^{-8} , corresponding to a significance of 5.5 standard deviations.

PACS numbers: 14.65.Ha; 12.15.Ji; 13.85.Qk

Within the standard model (SM), top quarks are produced through two different types of interactions at hadron colliders. The largest yield is from $t\bar{t}$ pairs, produced via the strong interaction [1]. Pair production was used by the D0 and CDF collaborations to establish the existence of the top quark in 1995 [2, 3]. The second source of top quarks is the electroweak production of single top quarks, observed by the D0 and CDF collaborations in 2009 [4, 5]. The single top quark production

rate is about half that for $t\bar{t}$ pairs and the signal-to-background ratio is worse, so the observation of this process is more difficult.

At the Tevatron, single top quarks are produced through W boson exchange, and accompanied by a b quark in the s channel ($t\bar{b} + \bar{t}b = tb$) [6], or by both a b and a light quark in the t -channel ($tq\bar{b} + \bar{t}qb = tqb$) [7, 8]. A third process, usually called “associated production,” in which the top quark is produced together with a W boson, has negligible cross section at the Tevatron [9]. Prior D0 and CDF publications [4, 5] measured the production cross section for the sum of tb and tqb while assuming the relative rate between the two processes as predicted by the SM. This relative rate, however, departs from the SM prediction in several new physics scenarios, for example, in models with additional quark generations [10], new heavy bosons [11], flavor-

*with visitors from ^aAugustana College, Sioux Falls, SD, USA, ^bThe University of Liverpool, Liverpool, UK, ^cSLAC, Menlo Park, CA, USA, ^dUniversity College London, London, UK, ^eCentro de Investigacion en Computacion - IPN, Mexico City, Mexico, ^fECFM, Universidad Autonoma de Sinaloa, Culiacán, Mexico, and ^gUniversität Bern, Bern, Switzerland. ^hVisitor from ETH-Zurich

changing neutral currents (FCNC) [12], or anomalous top quark couplings [13–15]. It is therefore of interest to measure the tb and tqb production cross sections separately, using a methodology that is independent of theoretical assumptions about their relative rates [11]. Furthermore, measuring the production rates of the two single top quark production modes to a precision comparable to that of the $t\bar{t}$ pair cross section not only tests the validity of the parton distribution functions of the proton and antiproton, but also the Cabibbo-Kobayashi-Maskawa (CKM) matrix elements [16] and higher-order corrections from quantum chromodynamics. These high-precision comparisons are important to check the self-consistency of the standard model (SM).

This Letter builds on the techniques developed by the D0 collaboration for prior measurements of single top quark production [4, 17–19], and analyzes a larger dataset corresponding to an integrated luminosity of 5.4 fb^{-1} . Using improved multivariate analysis (MVA) techniques, we report a new measurement of the tqb production rate that makes no assumptions about the tb production rate, and is therefore sensitive to various new physics scenarios.

The data for this analysis were collected with a logical OR of many trigger conditions that results in a fully efficient trigger selection for the single top quark signal. Electron, muon, missing transverse energy (\cancel{E}_T), and jet reconstruction algorithms used in this analysis have been described elsewhere [18, 20]. Events are selected that contain one jet with transverse momentum $p_T > 25 \text{ GeV}$ and at least a second jet with $p_T > 15 \text{ GeV}$, both within pseudorapidity $|\eta| < 3.4$. Events with 2, 3 or 4 jets are used in the analysis. Events are also required to contain exactly one isolated high- p_T electron or muon that originates from the $p\bar{p}$ interaction vertex and satisfies the following acceptance criteria: for the electron $|\eta| < 1.1$ and $p_T > 15(20) \text{ GeV}$ for events with 2 (3 or 4) jets; for the muon $|\eta| < 2.0$ and $p_T > 15 \text{ GeV}$. The \cancel{E}_T is required to be in the range of (20, 200) GeV for events with 2 jets and (25, 200) GeV for events with 3 or 4 jets.

The main background contributions arise from W bosons produced in association with jets, $t\bar{t}$ pairs, and multijet production in which a jet with high electromagnetic content mimics an electron, or a muon contained within a jet originating from the decay of a heavy-flavor quark (b or c quark) appears isolated. Diboson (WW , WZ , ZZ) and Z +jets processes add small additional contributions to the background. To limit the number of events originating from multijet production that enter our candidate samples through \cancel{E}_T mismeasurements, we require the \cancel{E}_T to be not aligned with or opposing the direction of the lepton or the leading jet and require high total scalar transverse energy of the lepton, jets and \cancel{E}_T (H_T). Additional requirements are placed on the transverse energy of all jets in all events and the second leading jet p_T in two-jet events to suppress soft-scattering

background.

To enhance the fraction of signal events in data, one or two of the jets in each event are required to originate from the hadronization of long-lived b hadrons, as inferred from a neural network b -tagging algorithm (“ b -tagged jet”) [21]. The data are divided into six mutually-exclusive subsamples to take advantage of different signal-to-background ratios and different sources of background. This separation is based on jet multiplicity (2, 3, or 4 jets), and on the number of b -tagged jets (1 or 2 b -tags). The signal acceptance of all selections corresponds to $(2.0 \pm 0.3)\%$ for tqb and $(2.9 \pm 0.4)\%$ for tb production, as estimated using Monte Carlo (MC) simulations.

Single top quark signal events are modeled using the COMHEP-based MC event generator SINGLETOP [22]. The kinematics of the generated events closely match those predicted by next-to-leading-order (NLO) calculations [23]. PYTHIA [24] is used to model the hadronization of all generated partons. The $t\bar{t}$, W +jets, and Z +jets backgrounds are simulated using the ALPGEN leading-log MC event generator [25], with PYTHIA used to model hadronization. The $t\bar{t}$ background is normalized to the predicted cross section [1] for a top quark mass of 172.5 GeV . The normalization of the W/Z backgrounds is obtained by scaling the ALPGEN cross sections to account for NLO effects [26]. Diboson backgrounds are modeled using PYTHIA.

The presence of additional $p\bar{p}$ interactions is modeled by events selected from random beam crossings matching the instantaneous luminosity profile in the data. All MC events are passed through a GEANT-based simulation [27] of the D0 detector. Small corrections, derived using samples depleted of single top quark events, are applied to all reconstructed objects to improve the agreement between data and simulation. In particular, any mismodeling of the pseudorapidity of jets or of the angular separation between the two leading jets in the W +jets sample is adjusted by reweighting the MC.

The multijet background is modeled using data containing non-isolated leptons. In the electron channel, the transverse momentum distribution of the lepton is reweighted to match the distribution in background events that pass the candidate-selection criteria. To increase the statistics in the muon channel, the jet closest to the muon is removed and the \cancel{E}_T recalculated. The overall normalization of the W +jets and the multijet backgrounds is obtained by comparing the background expectation to data in three sensitive variables: lepton transverse momentum, \cancel{E}_T , and the transverse mass of the W boson. This normalization is found after subtracting the contributions from the small backgrounds ($t\bar{t}$, Z +jets, and dibosons), before b -tagging, when the expected signal-to-background ratio (S:B) for the entire sample is $S:B \approx 1:279$.

The probability for the b -tagging algorithm to identify

a jet as originating from a b quark is measured in a sample of data with jets containing muons and compared to the corresponding efficiency measured in a MC sample. From this comparison we derive correction factors that we parametrize as a function of jet flavor, p_T , and η and apply to all the MC samples used in this analysis. After b -tagging, we check the normalization of the $Wb\bar{b}$ and $Wc\bar{c}$ samples in a sample that has no overlap with the one used in the single top quark cross section measurement and find the normalization to be consistent with unity. We assign a 12% uncertainty on the normalization of the $Wb\bar{b}$ and $Wc\bar{c}$ samples to account for variations in the Wcj ($j = u, d, s$) cross section and the $Wb\bar{b}$ to $Wc\bar{c}$ cross section ratio used in this study.

We consider systematic uncertainties that arise from the theoretical and detector modeling of the background processes and from the subsequent corrections applied to that model. Most uncertainties affect only the normalization of the distributions, but the corrections for the jet energy scale (JES), the jet energy resolution (JER), and the reweighting of the kinematic distributions in W +jets events also modify the differential distributions. The largest uncertainties come from the JER, corrections to the b -tagging efficiency, and the corrections for the jet-flavor composition in W +jets events, with smaller contribution from JES, MC statistics, integrated luminosity, and trigger uncertainties. The total systematic uncertainty on the background is 11%.

We select 8,471 events and expect 238 ± 28 tqb events. This corresponds to a S:B of approximately 1:33 for the sample with 1 b -tag and 1:50 for the sample with 2 b -tags. Table I lists the number of events expected and observed for each process as a function of jet multiplicity. We also define two control samples to check the background model components separately for the two main backgrounds: W +jets and $t\bar{t}$. The W +jets-dominated sample has low H_T , exactly two jets, and only one b -tagged jet. The $t\bar{t}$ -dominated sample has high H_T , exactly four jets, and one or two b -tagged jets. We find good agreement for both normalization and shape in most of distributions studied for the cross-check samples and also for the candidate sample before b -tagging, when the signal contribution is negligible.

We further improve the discrimination between signal and background by employing MVA techniques as described in [18]. We use two of our previous methods: boosted decision trees (BDT) [28] and Bayesian neural networks (BNN) [29]. In addition, we use a third method, neuroevolution of augmented topologies (NEAT) [30]. All three methods use the same data and background model, consider the same sources of systematic uncertainty, and rely on variables with signal-background discrimination power chosen from a common set of well modeled variables from five categories [31, 32]: single object kinematics, global event kinematics, jet reconstruction, top quark reconstruction, and angular

TABLE I: Number of expected and observed events in 5.4 fb^{-1} of integrated luminosity, with uncertainties including both statistical and systematic components. The $t\bar{t}$ and tqb contributions are normalized to their SM expectations.

Source	2 jets	3 jets	4 jets
$t\bar{t}$	104 ± 16	44 ± 7.8	13 ± 3.5
tqb	140 ± 13	72 ± 9.4	26 ± 6.4
$t\bar{t}$	433 ± 87	830 ± 133	860 ± 163
W +jets	$3,560 \pm 354$	$1,099 \pm 169$	284 ± 76
Z +jets & dibosons	400 ± 55	142 ± 41	35 ± 18
Multijets	277 ± 34	130 ± 17	43 ± 5.2
Total prediction	$4,914 \pm 558$	$2,317 \pm 377$	$1,261 \pm 272$
Data	4,881	2,307	1,283

correlations. The BDT method uses a common set of 50 variables for all analysis channels, while the NEAT method uses the TMVA implementation of the “RuleFit” algorithm [33, 34] to select the 30 most sensitive kinematic variables in each channel. New for this analysis, the BNN method constructs a discriminant using the lepton and jet 4-vectors, the \cancel{E}_T 2-vector, and variables that include lepton charge and b -tagging information, for a total of 14, 18 and 22 variables for events with 2, 3 and 4 jets.

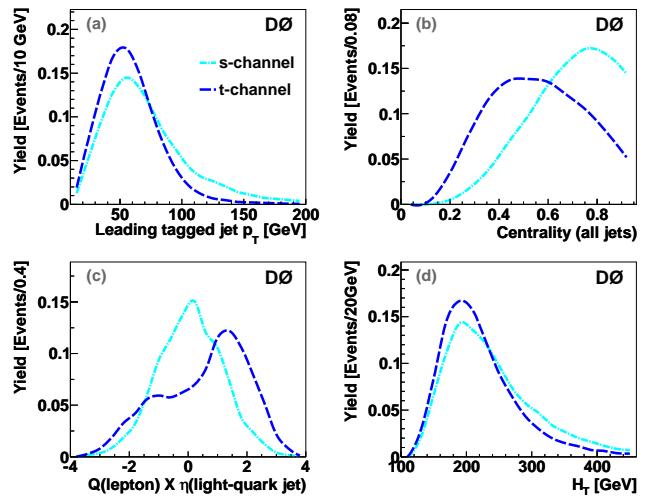


FIG. 1: Distribution for $t\bar{t}$ and tqb processes for (a) transverse momentum of the leading b -tagged jet, (b) centrality, defined as the ratio of the scalar sum of the p_T of the jets to the scalar sum of the energy of the jets in the event, (c) lepton charge multiplied by the leading non- b -tagged quark jet pseudorapidity and (d) total transverse energy. All the distributions are normalized to unity.

Each method is optimized to maximize the sensitivity to the tqb signal by treating the $t\bar{t}$ process as a background component with normalization given by the SM cross section [9]. Figure 1 shows the distributions of some of the variables that provide the greatest discrimination between the tqb and $t\bar{t}$ processes. To further

improve the sensitivity, the analyses are performed separately on the six mutually exclusive subsamples defined before. For all three methods the output variables are saved in histograms with a binning chosen to ensure that there are enough events to limit the uncertainties due to MC statistics.

Even though the three MVA techniques use the same data sample, they are only $\approx 70\%$ correlated with each other. We therefore combine these methods using an additional BNN algorithm (BNNComb) that takes as input the individual output discriminants of the BDT, BNN, and NEAT methods, and produces a single combined output discriminant. Figure 2 shows comparisons between the t -channel signal, the background model, and data for the combined discriminant, which leads to a more precise measurement of the cross section.

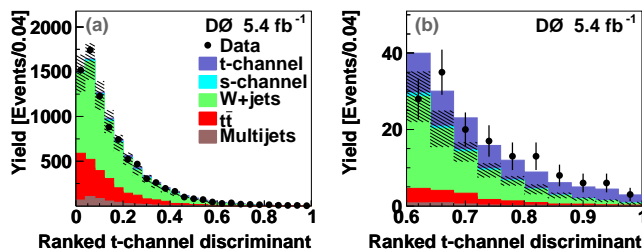


FIG. 2: Comparison of the signal and background models to data for the combined t -channel discriminant for (a) the entire discriminant range and (b) the signal region. The bins have been ordered by their expected S:B. The single top quark contributions are normalized to the measured cross sections. The t -channel contribution is visible above the hatched bands that show the uncertainty on the background prediction.

The single top quark production cross section is measured using a Bayesian approach as in [4, 17, 18]. We follow the approach of [19] and construct a two-dimensional (2D) posterior probability density as a function of the cross sections for the tqb and tb processes. The output discriminants for the signals, backgrounds, and data are used to form a binned likelihood as a product over all six analysis channels and all bins. No constraint is imposed on the relative rates of tb and tqb production. We assume a Poisson distribution for the observed number of events and uniform prior probabilities with positive values for the two signal cross sections. We integrate over the systematic uncertainties which are described by Gaussian priors that preserve the correlations between bins and channels. The tqb cross section is then extracted from a one-dimensional posterior probability density obtained from this 2D posterior by integrating over the tb axis, thus not making any assumptions about the value of the s -channel cross section. Similarly, the tb cross section is obtained by integrating over the tqb axis. Ensembles of datasets generated at several different cross section values are used to verify the linearity of the cross section extraction

procedure.

Figure 3 shows the 2D posterior probability density for the combined discriminant together with predictions from the SM [9] and various beyond-the-SM scenarios: four-quark-generations with CKM matrix element $|V_{ts}| = 0.2$ [10], top-flavor model with new heavy bosons at a scale $m_x = 1$ TeV [11], and FCNC with an up-quark/top-quark/gluon coupling $\kappa_u/\Lambda = 0.036$ [12].

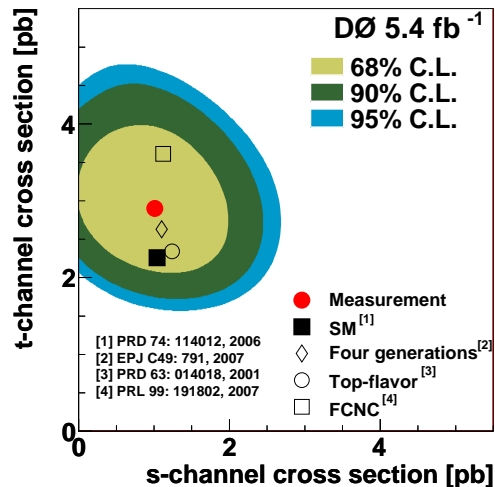


FIG. 3: Posterior probability density for tqb vs tb single top quark production in contours of equal probability density. The measured cross section and various theoretical predictions are also shown.

The measured cross sections of $\sigma(p\bar{p} \rightarrow tqb + X) = 2.90 \pm 0.59$ pb and $\sigma(p\bar{p} \rightarrow tb + X) = 0.98 \pm 0.63$ pb are in good agreement with the SM expectation for a top quark mass of 172.5 GeV [9]. The uncertainty includes both statistical and systematic sources. The cross section for t -channel single top quark production is the most precise measurement of an individual single top quark production channel to date with an uncertainty of 20%.

The significance of the t -channel cross section measurement is computed using a log-likelihood ratio approach [5, 19] which tests the compatibility of the data with two hypotheses: a null hypothesis where there is only background and a background plus signal hypothesis, where the number of signal events corresponds to the theoretical cross section. New for this analysis is the computation of the distributions for these two hypotheses given by an asymptotic Gaussian approximation [35]. With this approximation we compute for the first time, the significance of the measured tqb cross section independently of any assumption on the production rate of tb . We estimate the probability of the background to fluctuate and produce a signal as large as the one observed to be 1.6×10^{-8} , corresponding to a significance of 5.5 standard deviations (SD). The expected significance is 4.6 SD.

The presence of the t -channel signal is visible in

Fig. 4, which shows comparisons between the data, the background model, and the t -channel signal for a sample selected with $S:B > 0.32$ using the combined discriminant. Four kinematic variables with large discriminating power for t -channel single top quark production are shown: H_T , the reconstructed top quark mass, the lepton charge multiplied by the pseudorapidity of the leading non- b -tagged jet, and the t -channel spin correlation in the optimal basis [32, 36], i.e., the cosine of the angle between the light quark jet and the lepton, both in the reconstructed top quark rest frame.

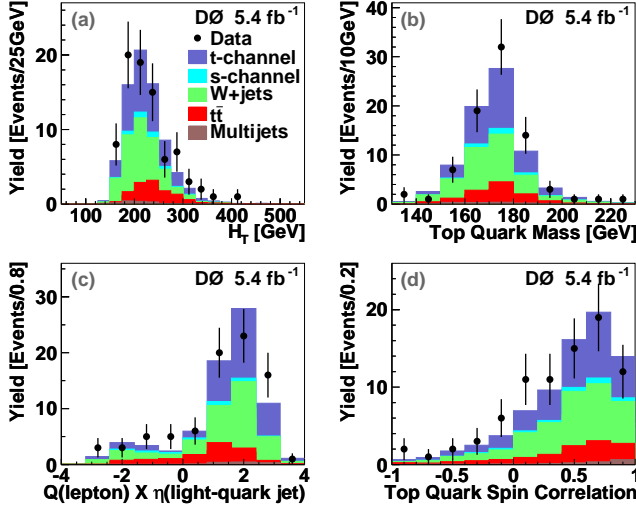


FIG. 4: (a) Total transverse energy, (b) reconstructed top quark mass, (c) lepton charge multiplied by the leading non- b -tagged quark jet pseudorapidity, and (d) t -channel top quark spin correlation (see text) for a sample selected with $S:B > 0.32$ using BNNComb discriminant. The t -channel and s -channel contributions have been normalized to their measured cross sections.

The measured cross section depends on the assumed mass of the top quark, m_t . The dependence is studied by repeating the analysis on MC samples generated at different values of m_t . Table II summarizes the measured cross section for different top quark masses.

TABLE II: Variation of the measured cross section for tqb and tb single top quark production with the top quark mass.

m_t	170 GeV	172.5 GeV	175 GeV
tqb	$2.80^{+0.57}_{-0.61}$	$2.90^{+0.59}_{-0.59}$	$2.53^{+0.58}_{-0.57}$
tb	$1.31^{+0.77}_{-0.74}$	$0.98^{+0.62}_{-0.63}$	$0.65^{+0.51}_{-0.50}$

In summary, we have presented a model-independent measurement of the t -channel single top quark production cross section using 5.4 fb^{-1} of integrated luminosity recorded by the D0 experiment at the Fermilab Tevatron accelerator. For a top quark mass of $m_t = 172.5 \text{ GeV}$, the measured cross section is $\sigma(p\bar{p} \rightarrow tqb + X) = 2.90 \pm 0.59 \text{ pb}$. This is the most precise measurement to date, and is in good agreement

with SM expectations.

We thank the staffs at Fermilab and collaborating institutions, and acknowledge support from the DOE and NSF (USA); CEA and CNRS/IN2P3 (France); FASI, Rosatom and RFBR (Russia); CNPq, FAPERJ, FAPESP and FUNDUNESP (Brazil); DAE and DST (India); Colciencias (Colombia); CONACyT (Mexico); KRF and KOSEF (Korea); CONICET and UBACyT (Argentina); FOM (The Netherlands); STFC and the Royal Society (United Kingdom); MSMT and GACR (Czech Republic); CRC Program and NSERC (Canada); BMBF and DFG (Germany); SFI (Ireland); The Swedish Research Council (Sweden); and CAS and CNSF (China).

- [1] S. Moch and P. Uwer, Phys. Rev. D **78**, 034003 (2008). At $m_t = 172.5 \text{ GeV}$, $\sigma(p\bar{p} \rightarrow t\bar{t} + X) = 7.46 \text{ pb}$.
- [2] F. Abe *et al.* (CDF Collaboration), Phys. Rev. Lett. **74**, 2626 (1995).
- [3] S. Abachi *et al.* (D0 Collaboration), Phys. Rev. Lett. **74**, 2632 (1995).
- [4] V. M. Abazov *et al.* (D0 Collaboration), Phys. Rev. Lett. **103**, 092001 (2009).
- [5] T. Aaltonen *et al.* (CDF Collaboration), Phys. Rev. Lett. **103**, 092002 (2009).
- [6] S. Cortese and R. Petronzio, Phys. Lett. B **253**, 494 (1991).
- [7] S. S. D. Willenbrock and D. A. Dicus, Phys. Rev. D **34**, 155 (1986).
- [8] C.-P. Yuan, Phys. Rev. D **41**, 42 (1990).
- [9] N. Kidonakis, Phys. Rev. D **74**, 114012 (2006). The cross sections for the single top quark processes ($m_t = 172.5 \text{ GeV}$) are $1.04 \pm 0.04 \text{ pb}$ (s -channel) and $2.26 \pm 0.12 \text{ pb}$ (t -channel).
- [10] J. Alwall *et al.*, Eur. Phys. J. C **49**, 791 (2007).
- [11] T. Tait and C.-P. Yuan, Phys. Rev. D **63**, 014018 (2001).
- [12] V. M. Abazov *et al.* (D0 Collaboration), Phys. Rev. Lett. **99**, 191802 (2007).
- [13] A. P. Heinson, A. S. Belyaev, and E. E. Boos, Phys. Rev. D **56**, 3114 (1997).
- [14] V. M. Abazov *et al.* (D0 Collaboration), Phys. Rev. Lett. **101**, 221801 (2008).
- [15] V. M. Abazov *et al.* (D0 Collaboration), Phys. Rev. Lett. **102**, 092002 (2009).
- [16] N. Cabibbo, Phys. Rev. Lett. **10**, 531 (1963); M. Kobayashi and T. Maskawa, Prog. Theor. Phys. **49**, 652 (1973).
- [17] V. M. Abazov *et al.* (D0 Collaboration), Phys. Rev. Lett. **98**, 181802 (2007).
- [18] V. M. Abazov *et al.* (D0 Collaboration), Phys. Rev. D **78**, 012005 (2008).
- [19] V. M. Abazov *et al.* (D0 Collaboration), Phys. Lett. B **682**, 363 (2010).
- [20] V. M. Abazov *et al.* (D0 Collaboration), Nucl. Instrum. Methods Phys. Res. Sect. A **565**, 463 (2006).
- [21] V. M. Abazov *et al.* (D0 Collaboration), Nucl. Instrum. Methods in Phys. Res. Sect. A **620**, 490 (2010).
- [22] E. E. Boos *et al.*, Phys. Atom. Nucl. **69**, 1317 (2006). We used SINGLETOP version 4.2p1.
- [23] Z. Sullivan, Phys. Rev. D **70**, 114012 (2004).

- [24] T. Sjöstrand, S. Mrenna, and P. Skands, J. High Energy Phys. **05**, 026 (2006). We used PYTHIA version 6.409.
- [25] M. L. Mangano *et al.*, J. High Energy Phys. **07**, 001 (2003). We used ALPGEN version 2.11.
- [26] R. K. Ellis, Nucl. Phys. Proc. Suppl. **160**, 170 (2006). We used MCFM version 5.1.
- [27] R. Brun and F. Carminati, CERN Program Library Long Writeup, Report No. W5013, 1993.
- [28] L. Breiman *et al.*, *Classification and Regression Trees* (Wadsworth, Stamford, 1984).
- [29] R. M. Neal, *Bayesian Learning for Neural Networks* (Springer-Verlag, New York, 1996).
- [30] K. O. Stanley and R. Miikkulainen, Evolutionary Computation **10**, 99 (2002).
- [31] Q.-H. Cao, R. Schwienhorst, and C.-P. Yuan, Phys. Rev. D **71**, 054023 (2005);
- [32] Q. H. Cao *et al.*, Phys. Rev. D **72**, 094027 (2005).
- [33] A. Hoecker, P. Speckmayer, J. Stelzer, J. Therhaag, E. von Toerne, and H. Voss, “TMVA: Toolkit for Multivariate Data Analysis,” PoS ACAT 040 (2007) [physics/0703039].
- [34] J. H. Friedman and B. E. Popescu, Ann. Appl. Stat. **2**, 916 (2008).
- [35] G. Cowan, K. Cranmer, E. Gross and O. Vitells, Eur. Phys. J. C **71**, 1554 (2011).
- [36] G. Mahlon and S. J. Parke, Phys. Rev. D **55**, 7249 (1997).